Article | Received 25 April 2025; Accepted 30 July 2025; Published 7 August 2025
https://doi.org/10.55092/bi20250004

Distinct nuclear and cytoplasmic transcriptomic signatures reveal-transcription alone is insufficient to determine glucose-induced transcriptomic dynamics

Atefeh Bagheri[1,2], Jinsil Kim[3,*] and Peng Jiang[1,2,*]

[1] Center for Gene Regulation in Health and Disease, Cleveland State University, Cleveland OH 44115, USA
[2] Department of Biological, Geological and Environmental Sciences, Cleveland State University, Cleveland OH 44115, USA
[3] Department of Biological Sciences, Biola University, La Mirada CA 90639, USA

* Correspondence authors; E-mails: jinsil.kim@biola.edu (J.K.); p.jiang@csuohio.edu (P.J.).

Highlights:

- Nuclear and cytoplasmic transcriptomes exhibit markedly different responses to glucose, indicating that transcription alone cannot explain mRNA abundance changes.
- Glucose-induced alternative splicing events are highly compartment- and cell type-specific, with minimal overlap between nuclear and cytoplasmic splicing patterns.
- Isoform abundance is not uniformly distributed between the nucleus and cytoplasm under normal conditions, suggesting selective export or stability mechanisms.
- Splicing changes in response to glucose do not correlate across compartments, underscoring the layered complexity of post-transcriptional regulation.
- This study introduces a subcellular transcriptomic profiling framework to disentangle transcriptional and post-transcriptional contributions to metabolic responses.

Abstract: Glucose profoundly influences cellular transcriptomes, but whether these changes are primarily driven by transcription remains unclear. Traditional bulk RNA sequencing, which interrogates total mRNA from whole cells, obscures distinct dynamics of nuclear and cytoplasmic transcriptomes. Nuclear RNA levels primarily reflect transcriptional activity but are also influenced by nuclear export, whereas cytoplasmic RNA abundances result from transcription, nuclear export, RNA stability (*i.e.*, RNA half-life), and active RNA degradation mechanisms. In this study, we systematically investigate glucose-induced transcriptomic responses in a subcellular location-and cell type-specific manner using three cell lines: FHC (normal colonic epithelial cells), MCF10A (normal breast epithelial cells), and MCF7 (metastatic breast cancer cells). Our findings reveal that, although nuclear and cytoplasmic mRNA levels show strong global correlations, glucose-induced changes in mRNA abundance exhibit minimal concordance between the nucleus and cytoplasm. Additionally, glucose-induced changes in exon inclusion levels often diverge between the nucleus and cytoplasm, underscoring the importance of post-transcriptional processes in shaping the cytoplasmic transcriptome response to glucose level changes. Glucose-induced differentially expressed

Copyright©2025 by the authors. Published by ELSP. This work is licensed under Creative Commons Attribution 4.0 International License, which permits unrestricted use, distribution, and reproduction in any medium provided the original work is properly cited.

genes (DEGs) and differentially spliced exons (ΔPSI) are enriched in distinct pathways exhibiting unique enrichment patterns depending on the subcellular location and cell line. These findings underscore the complexity of glucose-induced transcriptomic regulation, demonstrating that transcription alone is insufficient to explain the observed dynamics.

Keywords: nucleus; cytoplasm; mRNA levels; alternative splicing; transcriptomic dynamics

1. Introduction

Glucose is a key metabolic regulator that profoundly influences gene expression, impacting vital processes such as cell growth, proliferation, and survival [1]. While the transcriptional responses to glucose are well-documented [2], much less is understood about the role of post-transcriptional mechanisms—such as mRNA export, stability, and alternative splicing—in shaping the transcriptome. Traditional approaches to studying glucose-induced transcriptomic changes have largely relied on bulk RNA sequencing [3–5], which measures total mRNA levels without distinguishing between nuclear and cytoplasmic compartments. As mRNA must be exported from the nucleus to the cytoplasm for translation, nuclear mRNA abundance does not necessarily correlate with cytoplasmic mRNA levels. Moreover, post-transcriptional processes [6], including mRNA stability and alternative splicing, critically shape the functional mRNA pool in the cytoplasm.

Recent advances in subcellular location-specific transcriptomics have underscored the importance of separately analyzing nuclear and cytoplasmic transcriptomes to unravel the distinct regulatory mechanisms operating in each compartment [7,8]. However, few studies have systematically examined how glucose influences transcriptomic dynamics in a compartment-specific manner or whether these effects vary across different cell types.

In this study, we address these gaps by investigating the nuclear and cytoplasmic transcriptomic responses to glucose in three distinct cell lines: FHC (normal colonic epithelial cells), MCF10A (normal breast epithelial cells), and MCF7 (metastatic breast cancer cells). Through subcellular location-specific RNA sequencing and pathway enrichment analysis, we aim to disentangle the contributions of transcriptional and post-transcriptional regulation to glucose-induced transcriptomic changes.

Our findings reveal that glucose-induced changes in mRNA abundance exhibit minimal concordance between the nuclear and cytoplasmic compartments, highlighting the critical role of post-transcriptional processes such as mRNA export and stability in shaping nuclear and cytoplasmic transcriptomes. Furthermore, we demonstrate that glucose-induced alternative splicing changes are highly compartment-and cell type-specific, further emphasizing the complexity of transcriptomic regulation.

Pathway enrichment analysis reveals distinct biological pathways affected by glucose in a compartment-and cell type-specific manner. By dissecting the compartmental and cell type-specific transcriptomic responses to glucose, our study provides critical insights into the nuanced regulation of cellular metabolism and underscores the need for more targeted approaches in transcriptomic analysis.

2. Methods

2.1. Cell culture and treatment

The human colon epithelial cell line FHC, mammary gland epithelial cell line MCF 10A, and breast cancer cell line MCF7 were purchased from the American Type Culture Collection (ATCC, Manassas, VA). The FHC cells were cultured in DMEM/F-12 medium (Thermo Fisher Scientific, Waltham, MA) supplemented with 10% (v/v) bovine calf serum, additional 10 mM HEPES, 10 ng/ml cholera toxin, 5 µg/ml insulin, 5 µg/ml transferrin, 100 ng/ml hydrocortisone, and 20 ng/ml human recombinant EGF (MilliporeSigma, Burlington, MA). The MCF 10A cells were maintained in DMEM/F-12 medium supplemented with 5% (v/v) horse serum (Thermo Fisher Scientific, Waltham, MA), 100 ng/ml cholera toxin, 10 µg/ml insulin, 0.5 mg/ml hydrocortisone, and 20 ng/ml human recombinant EGF (MilliporeSigma, Burlington, MA). The MCF7 cells were maintained in DMEM medium (Thermo Fisher Scientific, Waltham, MA) supplemented with 10% (v/v) bovine calf serum (MilliporeSigma, Burlington, MA), 1% (v/v) nonessential amino acid and 1% (v/v) sodium pyruvate. All cells were cultured in media containing 100 units/ml penicillin and 100 µg/ml streptomycin (Thermo Fisher Scientific, Waltham, MA) at 37 °C in a humidified incubator with 5% CO_2. Cell media were replaced every 2–3 days and subcultured at 75%–80% confluency.

For glucose treatment, cells were plated in a 6-well plate and were allowed to adhere overnight in normal glucose media with 5 mM glucose. The next day, the media were replaced with fresh media containing either 5 mM glucose (low/normal glucose) or 25 mM glucose (high glucose). These concentrations mimic physiological normal and diabetic levels of glucose and were used in previous *in vitro* studies [6,9,10]. The normal- and high-glucose media were prepared by adding the same set of supplements as the culture media and two varying amounts of glucose to glucose-free basal media. Following the media change, the cells were incubated for 72 hours under normal culture conditions.

2.2. RNA extraction

After the incubation period of 72 hours, the cells were harvested for RNA extraction. Total RNA was isolated with on-column DNase I digestion using the E.Z.N.A.® Total RNA Kit I and the E.Z.N.A.® RNase-Free DNase I Set (Omega Bio-tek, Norcross, GA) according to the manufacturer's instructions. The nuclear and cytoplasmic RNA extraction with on-column DNA removal was conducted using the Cytoplasmic and Nuclear RNA Purification Kit and the RNase-Free DNase I Kit (Norgen Biotek, Thorold, Canada) following the manufacturer's instructions. The RNA extracted was stored at –80 °C until use. All RNA samples passed quality control for the purpose of RNA sequencing at the sequencing facility (Novogene, Sacramento, CA).

2.3. Quantitative real-time PCR (qRT-PCR)

The nuclear and cytoplasmic RNA extracted from MCF 10A cells was converted to cDNA with the High-Capacity cDNA Reverse Transcription Kit (Thermo Fisher Scientific, Waltham, MA). An equal amount of RNA (500 ng) from each fractionated sample was used as a template for reverse transcription in a 20 µl reaction volume, and the resulting cDNA was subjected to qRT-PCR analysis. Each sample was amplified in triplicate on the QuantStudio 6 Flex Real-Time PCR System using the Power SYBR Green PCR

Master Mix (Thermo Fisher Scientific, Waltham, MA) and forward and reverse primers for beta-actin (ACTB) according to the manufacturer's instruction. Data were presented as cycle threshold (Ct) values.

2.4. RNA library preparation and sequencing

Library preparation and sequencing were conducted by Novogene (Sacramento, CA). Briefly, messenger RNA was purified using poly-T oligo-attached magnetic beads, and after fragmentation, the first strand cDNA was synthesized using random hexamer primers, followed by the second strand cDNA synthesis. The remaining overhangs of double-stranded cDNA were converted into blunt ends via exonuclease/polymerase activities. After adenylation of the 3' end of the DNA fragments, sequencing adaptors were ligated to the cDNA, and the library fragments were purified with the AMPure XP system (Beckman Coulter, Brea, CA). The adaptor-ligated cDNA was then amplified using PCR, followed by purification of the PCR products. The quality of the library generated was assessed on the Agilent Bioanalyzer system, and sequencing was performed on an Illumina NovaSeq 6000 platform (Illumina, San Diego, CA) with 150-base-pair paired-end read lengths and more than 20 million read pairs generated per sample.

2.5. RNA-seq data analysis at gene level

RNA-seq Reads were mapped to the human genes (Ensembl v86) using Bowtie [11] allowing up to 3-mismatches and a maximum of 100 multiple hits. The gene expected read counts and the transcripts per million (TPMs) were estimated by RSEM [12]. TPMs were median-by-ratio normalized [13], and replicates were merged via calculating average normalized TPMs.

2.6. Differentially expressed genes (DEGs)

The EBSeq package [13] was used to assess the probability of gene expression (mRNAs) being differentially expressed between any two given conditions. We required that DEGs should have FDR < 5% via EBSeq and > 2 fold-change of "normalized read counts + 1".

2.7. Identification of differentially spliced exons

We used rMATS (replicate Multivariate Analysis of Transcript Splicing), a statistical method and tool to identify differential alternative splicing events from replicate RNA-Seq data [14]. This approach maps RNA-Seq reads to exon-exon junctions to quantify exon inclusion levels. rMATS employs a hierarchical framework to account for both estimation uncertainty within individual replicates and variability across replicates. In this study, we focused exclusively on cassette exons, a common type of alternative splicing event in which an exon can be either included or skipped in the mature transcript. Statistically significant differentially spliced exons were defined based on a false discovery rate (FDR) threshold of < 0.05 and a difference in exon inclusion levels exceeding 0.2.

3. Results

3.1. Discrepancy between nuclear and cytoplasmic mRNA abundance changes

Numerous studies have investigated how cells respond to changes in glucose levels, with most relying on bulk RNA sequencing, which typically measures mRNA levels in whole cells, encompassing both nuclear and cytoplasmic compartments. While mRNA is transcribed in the nucleus and subsequently exported to the cytoplasm for translation, it remains unclear whether changes in mRNA abundance in the nucleus directly correspond to changes in the cytoplasm. In this study we aim to explore the relationship between nuclear and cytoplasmic mRNA abundance changes and to determine whether these correlations are dependent on cell type. We analyzed three cell lines: FHC, MCF10A, and MCF7.

We first evaluated the integrity and purity of subcellular RNA fractions by quantifying ACTB (β-actin) mRNA, a well-established cytoplasmic marker [15], across cytoplasmic, nuclear, and total RNA fractions isolated from MCF10A cells. qPCR analysis (Supplementary Figure S1) revealed lower Ct values in the cytoplasmic (mean Ct = 15.7) and total RNA (mean Ct = 15.5) fractions compared to the nuclear fraction (mean Ct = 17.3), consistent with cytoplasmic enrichment of ACTB mRNA. Statistical analysis using Tukey's HSD post-hoc test confirmed significant differences between cytoplasmic and nuclear fractions (Q= 17.85, $p < 0.00001$), and between nuclear and total fractions (Q = 20.23, $p < 0.00001$), while no significant difference was observed between cytoplasmic and total fractions (Q = 2.38, p = 0.24474). These results validate the subcellular fractionation approach and confirm reliable separation of cytoplasmic and nuclear RNA.

We then evaluated the reproducibility of our RNA-seq data across replicates. As shown in Supplementary Figure S2, the Spearman's rank correlation coefficients between replicates were consistently ranged from 0.91 to 0.98, indicating high reproducibility. We then calculated Spearman's rank correlations to assess the relationship between nuclear and cytoplasmic mRNA relative abundance across the three cell lines under two conditions: normal glucose (5 mmol/L) and high glucose (25 mmol/L). The analysis revealed a strong global correlation between nuclear and cytoplasm.ic mRNA levels, with Spearman's correlation coefficient (Rho) exceeding 0.97 for all cell lines and conditions (Figure 1).

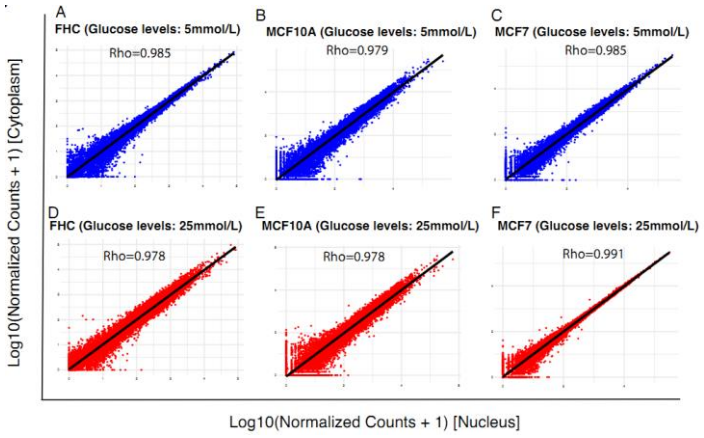

Figure 1. Spearman's rank correlations of mRNA abundance between the nucleus and cytoplasm: **(a)** FHC cell line with low glucose level; **(b)** MCF10A cell line with low glucose level; **(c)** MCF7 cell line with low glucose level; **(d)** FHC cell line with high glucose level; **(e)** MCF10A cell line with high glucose level; **(f)** MCF7 cell line with high glucose level.

Next, we investigated whether transcriptomic changes in the cytoplasm due to varying glucose levels reflected those observed in the nucleus. Surprisingly, our results showed poor correlation between glucose-induced changes in nuclear and cytoplasmic mRNA abundance (Figure 2). For instance, in the MCF7 cell line, while 74 genes were upregulated in the nucleus under high glucose compared to normal glucose, only one of these genes were similarly upregulated in the cytoplasm. Likewise, 57 genes were downregulated in the nucleus in response to high glucose, yet none were downregulated in the cytoplasm. In the MCF10A cell line, 33 genes were up-regulated under high glucose compared to normal glucose, with only one gene showing consistent changes in the cytoplasm. A detailed DEG list can be found in Supplementary Table S1. We further compared the log2-transformed fold-changes in gene expression responses to elevated glucose levels (low to high) between cytoplasmic and nuclear compartments (Supplementary Figure S3). This analysis revealed no substantial correlation (Spearman's Rho < 0.3 across all comparisons), further supporting our conclusion that the glucose-induced gene expression responses differ markedly between these two cellular compartments.

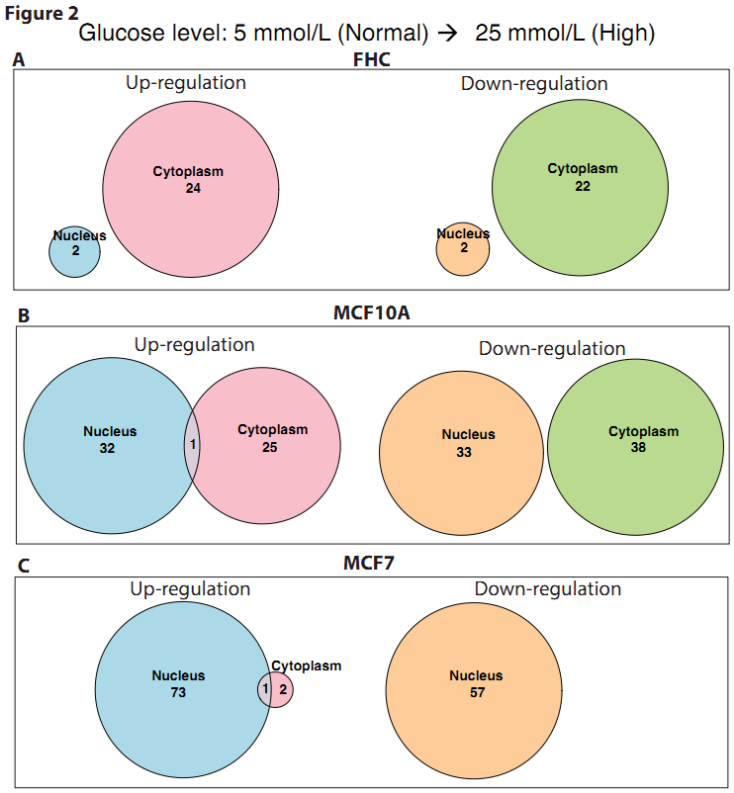

Figure 2. Overlap of upregulated and downregulated genes in response to glucose level changes between the nucleus and cytoplasm. The number of genes upregulated or downregulated in response to an increase in the glucose level from 5 mmol/L to 25 mmol/L for **(a)** FHC, **(b)** MCF10A, and **(c)** MCF7, are indicated in each venn diagram.

The observed discrepancy may be attributed to various factors influencing cytoplasmic mRNA levels beyond transcription, such as mRNA export, degradation, and stability. Our findings, which were consistent across all three cell lines, indicate that transcription alone does not account for glucose-induced changes in cytoplasmic mRNA abundance, and therefore, may not directly predict changes in protein levels.

3.2. Isoform abundance is unevenly distributed between the nucleus and cytoplasm at normal glucose condition (5 mmol/L)

Alternative splicing occurs in the nucleus, where a single pre-mRNA can give rise to multiple isoforms through RNA processing. If all isoforms have an equal chance of being exported from the nucleus to the cytoplasm, the relative abundance of each isoform would remain consistent between these two cellular compartments. In this study, we investigated whether the relative abundance of different isoforms is maintained between the nucleus and the cytoplasm. We utilized RNA-seq mapped reads to exon-exon junctions to estimate the relative abundance of isoforms and detect potential isoform abundance switches. Specifically, we compared isoforms containing a particular exon with those that skip it, employing a hierarchical framework to account for both estimation uncertainty within individual replicates and variability across replicates to detect alternative splicing changes between two conditions [14]. To quantify the relative abundance of isoforms containing a specific exon, we utilized PSI (Percent Spliced In), a metric that measures the proportion of transcripts that include a particular exon compared to those that exclude it. PSI values range from 0% to 100%, where 0% represents complete exon skipping, and 100% signifies full exon inclusion. For each comparison, significant splicing changes are defined as those with a PSI difference (ΔPSI) greater than 0.2 between two conditions and a false discovery rate (FDR) below 0.05. Notably, both increases and decreases in exon inclusion are observed across both cellular compartments (nucleus and cytoplasm). As shown in Figure 3A, an example exon exhibits a higher inclusion level in the cytoplasm compared to the nucleus in the FHC cell line. Specifically, this exon, located in the DAZ interacting zinc finger protein 1 like (*DZIP1L*) gene, which encodes a ciliary basal body protein localized to centrioles, has PSI values of 0.39 and 0.65 in two replicates of the nucleus. In contrast, its inclusion is significantly elevated in the cytoplasm, with PSI values of 0.78 and 0.78 across two replicates. These results suggest that the relative isoform abundance differs between the nucleus and cytoplasm. Figure 3B shows an example of decreased exon inclusion in the cytoplasm. This exon, which is located in the disco interacting protein 2 homolog C (*DIP2C*) gene whose alteration is associated with neurological disorders [16,17] and cancer [18] shows PSI values of 0.39 and 0.45 in the nucleus but drops to 0.07 and 0.26 in the cytoplasm, indicating that isoforms containing this exon are depleted in the cytoplasm compared to the nucleus.

In total, we detected 316 and 292 exons with higher inclusion levels in the cytoplasm and nucleus, respectively in FHC cells. To assess whether these isoform preferences in the cytoplasm *versus* nucleus are cell-type dependent or independent, we conducted a similar analysis in two other cell lines, MCF7 and MCF10A. As shown in Figures 3C and 3D, the isoform preferences appear largely cell-type dependent. For example, among the 316 exons with higher inclusion in the cytoplasm of FHC cells, only 20 exons also exhibit higher inclusion in the cytoplasm of MCF7 cells, and 15 exons in MCF10A cells (Figure 3C). Similarly, of the 292 exons with higher inclusion in the nucleus of FHC cells, only 18 exons show higher inclusion in the nucleus of MCF7 cells, and 10 exons in MCF10A cells (Figure 3D). These findings indicate that exon inclusion patterns in the cytoplasm and nucleus are not consistent across cell types, highlighting the cell-type specificity of isoform preference between the nucleus and cytoplasm. In addition to exon skipping ("cassette exons"), which represents the most prevalent type of alternative splicing event, other splicing patterns—including alternative 5′ splice sites, alternative 3′ splice sites, mutually exclusive exons, and retained introns—also display differential

splicing between the nucleus and cytoplasm (Supplementary Table S2), suggesting extensive compartment-specific isoform preferences.

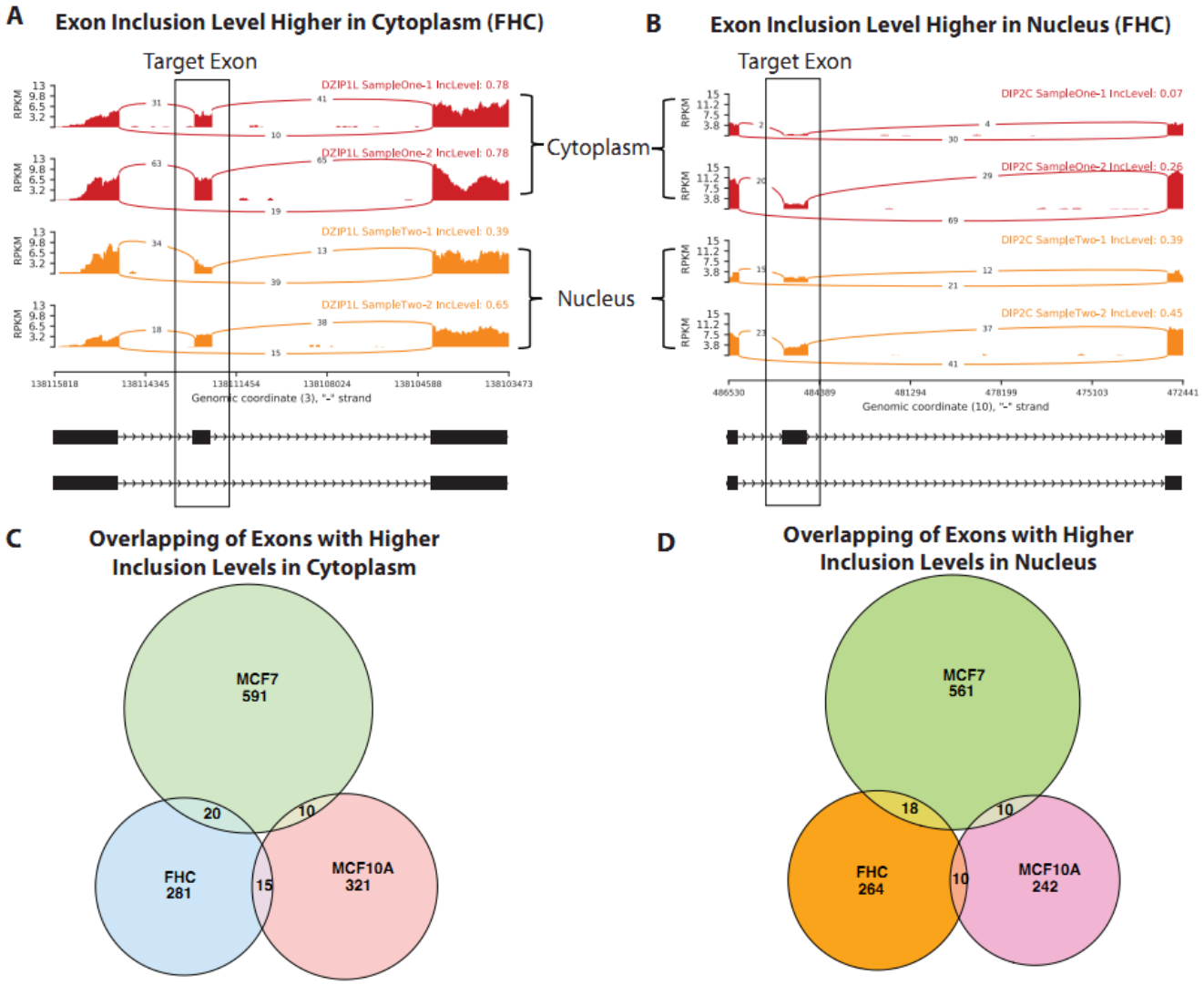

Figure 3. Exon inclusion levels are discordant between the nucleus and cytoplasm (normal glucose: 5 mmol/L): **(a)** An exon in *DZIP1L* whose inclusion level is higher in the cytoplasm compared with that in the nucleus in FHC cells; **(b)** An exon in *DIP2C* gene whose inclusion level is lower in the cytoplasm compared with that in the nucleus in FHC cells; **(c)** Overlapping of exons with higher inclusion levels in the cytoplasm compared with the nucleus among FHC, MCF10A, and MCF7 cell lines; **(d)** Overlapping of exons with higher inclusion levels in the nucleus compared with the cytoplasm among FHC, MCF10A, and MCF7 cell lines.

3.3. Glucose-induced exon inclusion level changes in the cytoplasm do not mirror those in the nucleus

We further investigated whether glucose-induced exon inclusion level changes observed in the nucleus are consistent with those in the cytoplasm. Across the FHC, MCF7, and MCF10A cell lines, we identified 642, 926, and 643 exons, respectively, that were differentially spliced between normal (5 mmol/L) and high (25 mmol/L) glucose levels in either the nucleus or the cytoplasm. Notably, the majority of these glucose-induced splicing changes were unique to either the nucleus or the cytoplasm,

with minimal overlap observed between compartments. For instance, only 44, 69, and 39 exons were found to be statistically significantly differentially spliced in both nuclear and cytoplasmic fractions in the FHC, MCF7, and MCF10A cell lines, respectively, under varying glucose levels. We further examined whether exons exhibiting statistically significant glucose-induced alternative splicing in both the nucleus and cytoplasm showed correlated changes in exon inclusion levels. As shown in Figure 4, glucose-induced exon inclusion changes in the nucleus and cytoplasm demonstrated minimal correlation. Specifically, the Spearman correlation coefficients (Rho) for the FHC, MCF7, and MCF10A cell lines were −0.176, 0.049, and 0.228, respectively. For instance, in the FHC cell line (Figure 4A), several exons exhibit substantial inclusion changes in the nucleus (high ΔPSI) but remain largely unchanged in the cytoplasm. A similar trend is observed for MCF7 and MCF10A cells (Figure 4B, 4C), where no consistent pattern emerges between the two cellular compartments. These findings suggest that glucose-induced alternative splicing in the nucleus and potential isoform selection during export to the cytoplasm jointly contribute to the complexity of post-transcriptional regulation.

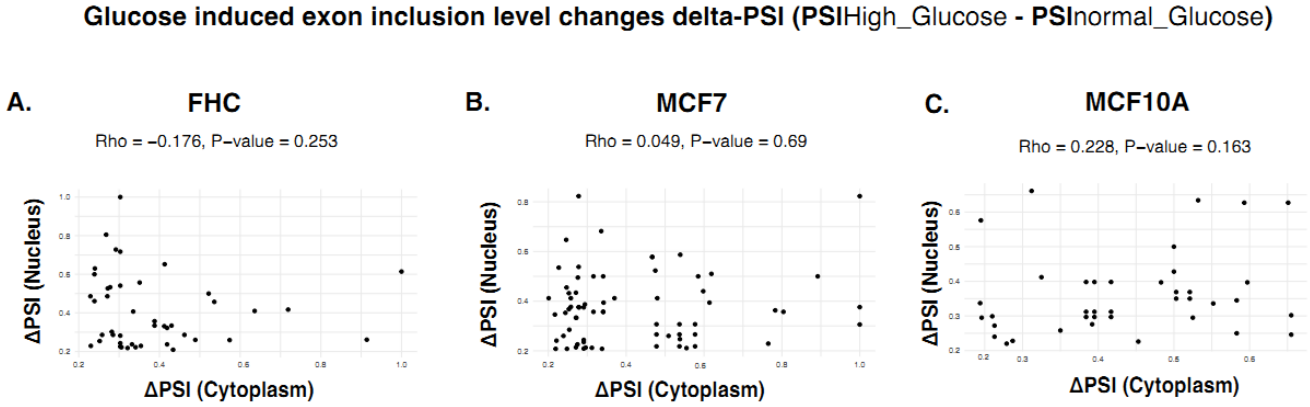

Figure 4. Spearman's rank correlations of glucose-induced changes in exon inclusion levels between the cytoplasm and nucleus. The Spearman's correlation coefficient (Rho) is shown for each of the FHC **(a)**, MCF10A **(b)** and MCF7 **(c)** cell lines.

3.4. Pathways enriched in glucose-induced gene-level and isoform-level changes are compartment- and cell type-dependent

To determine whether the enriched pathways associated with glucose-induced gene-level and isoform-level changes are dependent on cellular compartment and cell type, we compared enriched pathways on differentially expressed genes (DEGs) and genes with differentially spliced exons (ΔPSI) under normal (5 mmol/L) and high (25 mmol/L) glucose conditions across the FHC, MCF7, and MCF10A cell lines.

As shown in Figure 5A, pathways enriched by glucose-induced DEGs are highly depending on the cellular compartment (nucleus *vs.* cytoplasm) and cell types. For instance, the "HDL remodeling" pathway is only significantly enriched (FDR < 0.05) in the cytoplasm of MCF7 cells, but not in the nucleus or other cell types. Notably, pathways involved in lipid metabolism, immune signaling (e.g., "Interleukin-10 signaling"), and cell cycle regulation showed enrichment patterns that differed between the nucleus and cytoplasm, as well as across the three cell lines.

In contrast to DEGs, the pathways enriched by differentially spliced exons (ΔPSI) displayed a more limited but distinct pattern (Figure 5B). These splicing changes were highly dependent on both the

cellular compartment and the cell line. For example, in FHC cells, genes with alternative splicing under high glucose conditions enriched pathways related to “Transcriptional activation of p53 responsive genes”, “Transcriptional activation of cell cycle inhibitor p21”, and “Insulin-like Growth Factor-2 mRNA Binding Proteins (IGF2BPs)” in the nucleus while the cytoplasm of FHC cells and other cell types did not show such enrichment. This suggests that glucose-induced splicing changes may selectively impact pathways, with unique patterns in different cellular compartments and the cell types. While our current analysis does not include direct functional validation, future studies will aim to experimentally confirm the biological significance and functional implications of these compartment-and cell type-specific glucose-induced gene and isoform-level changes.

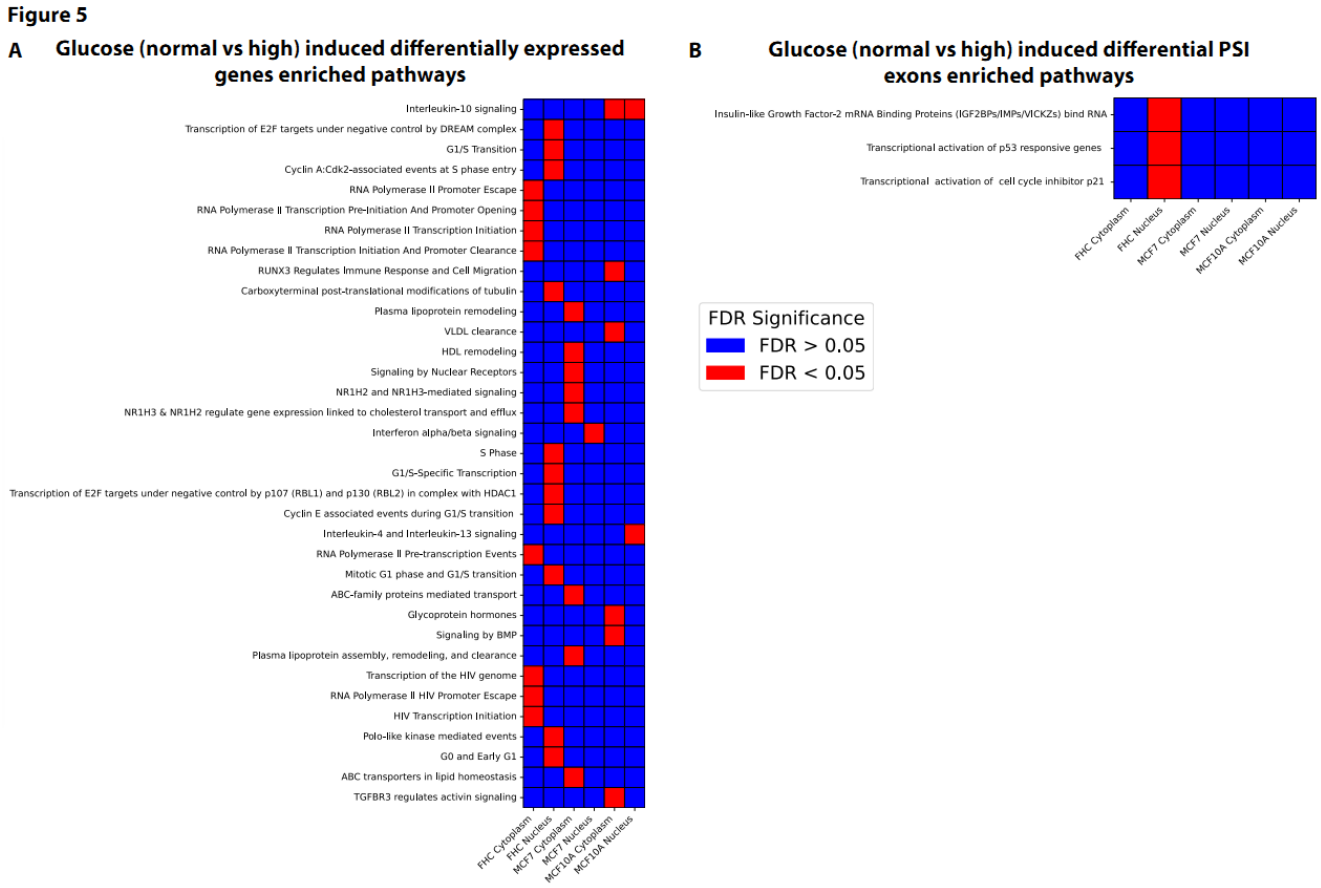

Figure 5. Pathway enrichment analysis of glucose-induced differentially expressed and differentially spliced genes: **(a)** Pathways enriched in glucose-induced differentially expressed genes; **(b)** Pathways enriched in genes with glucose-induced differentially spliced exons.

4. Discussions

Most transcriptomic studies rely on bulk RNA sequencing, which measures mRNA levels in whole cells without distinguishing between nuclear and cytoplasmic compartments. This approach assumes that transcriptomic responses are primarily transcriptional. However, our study provides a more nuanced perspective by separately analyzing nuclear and cytoplasmic transcriptomes. We demonstrated that glucose-induced changes in mRNA abundance show minimal concordance between these compartments, highlighting the critical role of post-transcriptional processes, such as mRNA export, stability, and degradation, in shaping the cytoplasmic transcriptome. This discrepancy underscores the

limitations of interpreting bulk RNA-seq data as purely reflective of transcriptional responses, as cytoplasmic mRNA levels are shaped by complex post-transcriptional regulatory mechanisms.

In addition to examining mRNA abundance, we explored differences in exon inclusion levels between the nucleus and cytoplasm. Our findings reveal that exon inclusion patterns are highly compartment- and cell-type specific. For example, some exons showed higher inclusion in the cytoplasm compared to the nucleus, while others were preferentially included in the nucleus. These differences were observed across the three cell lines: FHC, MCF10A, and MCF7, suggesting that alternative splicing and isoform selection during mRNA export contribute significantly to the transcriptomic diversity. Furthermore, glucose-induced changes in exon inclusion often diverged between the two compartments, emphasizing the distinct regulatory landscapes governing nuclear and cytoplasmic transcriptomes.

To investigate the relevance of glucose-induced differentially expressed genes (DEGs) to diabetes, we utilized *KinderMiner (https://skim.morgridge.org)*, a literature mining tool that queries the entire PubMed database for gene–disease associations. Notably, 28 of the DEGs showed significant associations with the term "diabetes," indicating strong literature support for their relevance (Supplementary Table S3). Interestingly, these diabetes-associated genes exhibited pronounced compartment-specific and cell type specific expression patterns, suggesting that distinct cellular compartments and specific cell types may play specialized roles in the response.

While our study primarily emphasizes the difference between the nuclear and cytoplasmic transcriptomes, several findings from our analyses are particularly intriguing. Notably, the HDL remodeling pathway was identified as enriched among the differentially expressed genes in the cytoplasmic compartment of MCF7 cells. HDL remodeling plays a crucial role in the maintenance of cellular cholesterol homeostasis by influencing the structure and metabolic turnover of HDL particles [19,20]. A recent study has shown that cholesterol levels have impact on multiple cellular phenotypes relevant to breast cancer development in MCF7 cells, including cell growth and expression of estrogen and progesterone receptors and cell proliferation markers such as Ki-67 [21]. A different study, using RNA-Seq analysis, by Ambrosio *et al.* has reported that the co-culture of MCF7 cells with adipocytes in a glucose-rich (25 mM glucose) environment determined a re-program of breast cancer cell transcriptome driving lipid accumulation, which is considered as a hallmark of breast cancer aggressiveness [22]. Given the findings of these studies and increasing implication of lipid- and cholesterol-associated pathways in cancer progression and chemotherapy response [23,24], it is speculated that altered cholesterol homeostasis in the cytoplasm of MCF7 cells through glucose-induced HDL remodeling may aggravate cancer-related phenotypes, which warrants experimental investigation.

We also observed compartment-specific splicing variations involving exons in genes such as *DZIP1L* and *DIP2C* in the cytoplasm of FHC cells. Currently, there is limited information available regarding the function of the *DZIP1L* gene except its role in ciliary initiation and morphogenesis and the integrity of the transition zone and its implication in polycystic kidney disease [25,26], making it challenging to elucidate the biological impact of its elevated exon inclusion in a high glucose environment. However, considering the frequent association of increased exon inclusion with higher overall gene expression [27], it may merit future investigation to determine whether the glucose-induced higher exon inclusion level leads to an increase in overall expression of *DZIP1L* and what functional consequences it might carry in the context of colorectal cells specifically. The *DIP2C* gene, which is widely expressed in the central nervous system and has been linked to neurodevelopmental disorders [17,28], has been

documented to be involved in cancer [18,29]. Specifically, its decreased expression level has been reported in subtypes of breast cancer [29], and its knockout in RKO colorectal cancer cells has been shown to lead to substantial DNA methylation and gene expression changes, cellular senescence, and epithelial-mesenchymal transition [18]. These studies suggest the possibility that the glucose-induced lower exon inclusion level may cause a decrease in *DIP2C* expression, which may promote or inhibit tumorigenesis by inducing changes in DNA methylation, gene expression, and cellular states and behaviors.

Several previous studies have used subcellular transcriptome analysis to investigate the profiles of nuclear and cytoplasmic transcripts in human brain cells and tissues. Price *et al.*, in their study of prenatal and adult cortical transcriptomes, observed more distinct nuclear and cytoplasmic transcript profiles in the adult cortex than the prenatal cortex with genes exhibiting decreasing expression during development preferentially retained in the nucleus, suggesting a role for nuclear retention in developmental regulation of the brain [30]. Another study that examined subcellular RNA fractions of brain tissues in combination with allele-specific expression analysis found that a substantial portion of genetic regulation of gene expression occurs post-transcriptionally in the cytoplasm [31]. While the context of our study is different from these studies, our findings of the differential gene expression and splicing between the two subcellular compartments similarly confirm the critical importance of post-transcriptional processes in the regulation of cellular responses to biological cues or environmental stimuli as well as the evident value of the subcellular transcriptome analysis in understanding the complexity of gene regulation in various contexts. In addition, as demonstrated in a previous study using compartment-specific transcript profiling to gain insight into the mechanisms of neuroinflammation [32], the application of the subcellular RNA distribution analysis can be extended to disease studies, shedding light on the molecular basis of pathologic conditions. On this basis, our study may lay the groundwork for subsequent research exploring glucose-related conditions.

While our study provides novel insights into the compartment-specific dynamics of glucose-induced transcriptomic changes, it is important to acknowledge its limitations. Our conclusions are based on glucose-induced conditions, and the extent to which these findings generalize to other stimuli or metabolic contexts remains uncertain. Additionally, we focused on three specific cell lines, which may not fully capture the diversity of transcriptomic responses across different cell types or tissues. Future studies could extend this analysis to other metabolic conditions and a wider range of cell types to determine whether the observed compartmental differences are universally applicable.

In summary, our study highlights the critical need for compartment-specific transcriptomic analyses to fully understand the regulatory complexity of glucose-induced cellular responses.

5. Supplementary data

The authors confirm that the supplementary data are available within this article.

Acknowledgments

We thank the support from the Center for Gene Regulation in Health and Disease (GRHD) at Cleveland State University and Anton Komar. This work was also supported by DARPA AWD00001593 (PJ) and research funding from Biola University (JK).

Authors' contribution

Conceptualization, Jinsil Kim and Peng Jiang; methodology, Peng Jiang; formal analysis, Atefeh Bagheri; investigation, Peng Jiang; resources, Jinsil Kim and Peng Jiang; data curation, Jinsil Kim; writing—original draft preparation, Peng Jiang; writing—review and editing, Peng Jiang and Jinsil Kim; supervision, Jinsil Kim and Peng Jiang; project administration, Jinsil Kim and Peng Jiang; funding acquisition, Jinsil Kim and Peng Jiang. All authors have read and agreed to the published version of the manuscript.

Data availability statement

We have submitted the RNA-seq data and the gene expression data (TPMs and Mapping counts) to GEO (accession number: GSE284924). For any questions regarding data access, please contact Peng Jiang (p.jiang@csuohio.edu).

Conflicts of interests

The authors declare no conflict of interest.

References

[1] Zhao Y, Wieman HL, Jacobs SR, Rathmell JC. Chapter twenty-two mechanisms and methods in glucose metabolism and cell death. *Methods Enzymol.* 2008, 442:439–457.

[2] Meugnier E, Rome S, Vidal H. Regulation of gene expression by glucose. *Curr. Opin. Clin. Nutr. Metab. Care* 2007, 10(4):518–522.

[3] Wang Z, Gerstein M, Snyder M. RNA-Seq: a revolutionary tool for transcriptomics. *Nat. Rev. Genet.* 2009, 10(1):57–63.

[4] Webert L, Faro D, Zeitlmayr S, Gudermann T, Breit A. Analysis of the glucose-dependent transcriptome in murine hypothalamic cells. *Cells* 2022, 11(4):639.

[5] Pang L, Wang Y, Zheng M, Wang Q, Lin H, *et al.* Transcriptomic study of high-glucose effects on human skin fibroblast cells. *Mol. Med. Rep.* 2016, 13(3):2627–2634.

[6] Corbett AH. Post-transcriptional regulation of gene expression and human disease. *Curr. Opin. Cell Biol.* 2018, 52:96–104.

[7] Hurni C, Weger BD, Gobet C, Naef F. Comprehensive analysis of the circadian nuclear and cytoplasmic transcriptome in mouse liver. *PLos Genet.* 2022, 18(8):e1009903.

[8] Zaghlool A, Niazi A, Bjorklund AK, Westholm JO, Ameur A, *et al.* Characterization of the nuclear and cytosolic transcriptomes in human brain tissue reveals new insights into the subcellular distribution of RNA transcripts. *Sci. Rep.* 2021, 11(1):4076.

[9] Dutta D, Ziemke M, Sindelar P, Vargas H, Lim JY, *et al.* Cytoarchitecture of breast cancer cells under diabetic conditions: role of regulatory kinases-rho kinase and focal adhesion kinase. *Cancers* 2024, 16(18):3166.

[10] Khawkhiaw K, Chomphoo S, Kunprom W, Thithuan K, Sorin S, *et al.* Involvement of interleukin-1β in high glucose-activated proliferation of cholangiocarcinoma. *Transl. Gastroenterol. Hepatol.* 2024, 9:36.

[11] Langmead B, Trapnell C, Pop M, Salzberg SL. Ultrafast and memory-efficient alignment of short DNA sequences to the human genome. *Genome Biol.* 2009, 10(3):R25.

[12] Li B, Dewey CN. RSEM: accurate transcript quantification from RNA-Seq data with or without a reference genome. *BMC Bioinf.* 2011, 12(1):323.

[13] Leng N, Dawson JA, Thomson JA, Ruotti V, Rissman AI, *et al.* EBSeq: an empirical Bayes hierarchical model for inference in RNA-seq experiments. *Bioinformatics* 2013, 29(8):1035–1043.

[14] Shen S, Park JW, Lu ZX, Lin L, Henry MD, *et al.* rMATS: robust and flexible detection of differential alternative splicing from replicate RNA-Seq data. *Proc. Natl. Acad. Sci. U.S.A.* 2014, 111(51):E5593–E5601.

[15] Nietmann P, Kaub K, Suchenko A, Stenz S, Warnecke C, *et al.* Cytosolic actin isoforms form networks with different rheological properties that indicate specific biological function. *Nat. Commun.* 2023, 14(1):7989.

[16] Yang L, Zhao S, Ma N, Liu L, Li D, *et al.* Novel DIP2C gene splicing variant in an individual with focal infantile epilepsy. *Am. J. Med. Genet. Part A* 2022, 188(1):210–215.

[17] Li Y, Sun C, Guo Y, Qiu S, Li Y, *et al.* DIP2C polymorphisms are implicated in susceptibility and clinical phenotypes of autism spectrum disorder. *Psychiatry Res.* 2022, 316:114792.

[18] Larsson C, Ali MA, Pandzic T, Lindroth AM, He L, *et al.* Loss of DIP2C in RKO cells stimulates changes in DNA methylation and epithelial-mesenchymal transition. *BMC Cancer* 2017, 17(1):487.

[19] Zannis VI, Fotakis P, Koukos G, Kardassis D, Ehnholm C, *et al.* HDL biogenesis, remodeling, and catabolism. *Handb Exp Pharmacol* 2015, 224:53–111.

[20] Paukner K, Kralova Lesna I, Poledne R. Cholesterol in the cell membrane-an emerging player in atherogenesis. *Int. J. Mol. Sci.* 2022, 23(1):533.

[21] Albi E, Mandarano M, Cataldi S, Ceccarini MR, Fiorani F, *et al.* The effect of cholesterol in mcf7 human breast cancer cells. *Int. J. Mol. Sci.* 2023, 24(6):5935.

[22] Ambrosio MR, Adriaens M, Derks K, Migliaccio T, Costa V, *et al.* Glucose impacts onto the reciprocal reprogramming between mammary adipocytes and cancer cells. *Sci. Rep.* 2024, 14(1):24674.

[23] Schiliro C, Firestein BL. Mechanisms of metabolic reprogramming in cancer cells supporting enhanced growth and proliferation. *Cells* 2021, 10(5):1056.

[24] Yang K, Wang X, Song C, He Z, Wang R, *et al.* The role of lipid metabolic reprogramming in tumor microenvironment. *Theranostics* 2023, 13(6):1774–1808.

[25] Lu H, Galeano MCR, Ott E, Kaeslin G, Kausalya PJ, *et al.* Mutations in DZIP1L, which encodes a ciliary-transition-zone protein, cause autosomal recessive polycystic kidney disease. *Nat. Genet.* 2017, 49(7):1025–1034.

[26] Wang C, Li J, Takemaru KI, Jiang X, Xu G, *et al.* Centrosomal protein Dzip1l binds Cby, promotes ciliary bud formation, and acts redundantly with Bromi to regulate ciliogenesis in the mouse. *Development* 2018, 145(6):dev164236.

[27] Karlebach G, Steinhaus R, Danis D, Devoucoux M, Anczukow O, *et al.* Alternative splicing is coupled to gene expression in a subset of variably expressed genes. *npj Genomic Med.* 2024, 9(1):54.

[28] Ha T, Morgan A, Bartos MN, Beatty K, Cogne B, *et al.* De novo variants predicting haploinsufficiency for DIP2C are associated with expressive speech delay. *Am. J. Med. Genet. Part A* 2024, 194(7):e63559.

[29] Li J, Ping J, Ma B, Chen Y, Li L. DIP2C expression in breast cancer and its clinical significance. *Pathol. Res. Pract.* 2017, 213(11):1394–1399.

[30] Price AJ, Hwang T, Tao R, Burke EE, Rajpurohit A, *et al.* Characterizing the nuclear and cytoplasmic transcriptomes in developing and mature human cortex uncovers new insight into psychiatric disease gene regulation. *Genome Res.* 2020, 30(1):1–11.

[31] D'Sa K, Guelfi S, Vandrovcova J, Reynolds RH, Zhang D, *et al.* Analysis of subcellular RNA fractions demonstrates significant genetic regulation of gene expression in human brain post-transcriptionally. *Sci. Rep.* 2023, 13(1):13874.

[32] Liao Y, Kuang C, Bao Z, He Y, Gu L, *et al.* Nucleo-cytoplasmic RNA distribution responsible for maintaining neuroinflammatory microenvironment. *RNA Biol.* 2021, 18(sup2):866–880.